Carbon metabolism-mediated myogenic differentiation

Abigail L. Bracha[1,8], **Arvind Ramanathan**[2,6,8], **Sui Huang**[5], **Donald E. Ingber**[1,4], and **Stuart L. Schreiber**[2,3,7]

[1] Vascular Biology Program, Departments of Pathology & Surgery, Children's Hospital and Harvard Medical School, Boston, Massachusetts 02115, USA

[2] Howard Hughes Medical Institute at the Broad Institute of Harvard and MIT, 7 Cambridge Center, Cambridge, Massachusetts 02142, USA

[3] Department of Chemistry and Chemical Biology, Harvard University, 12 Oxford Street, Cambridge, Massachusetts 02138, USA

[4] Wyss Institute for Biologically Inspired Engineering and School of Engineering and Applied Sciences, Harvard University, Cambridge, Massachusetts 02138, USA

[5] Institute for Biocomplexity and Informatics, University of Calgary, Calgary, Alberta T2N 1N4, Canada

Abstract

The role of nutrients and metabolism in cellular differentiation is poorly understood. Using RNAi screening, metabolic profiling and small-molecule probes, we discovered three metabolic enzymes whose knockdown induces differentiation of mouse C2C12 myoblasts even in the presence mitogens: phosphoglycerate kinase (Pgk1), hexose-6-phosphate dehydrogenase (H6pd) and ATP citrate lyase (Acl). These enzymes and the pathways they regulate provide novel targets for the control of myogenic differentiation in myoblasts and rhabdomyosarcoma cells.

Keywords

taurodeoxycholic acid (TUDCA); glycochenodeoxycholic acid; 3-phosphoglycerate; phosphoenol pyruvate (PEP); cyclosporin A (CsA); trichostatin A (TSA); pravastatin; atorvastatin; fluvastatin

[6]Correspondence should be addressed to A.R. (aramanat@broadinstitute.org). [7]Correspondence should be addressed to SLS (stuart_schreiber@harvard.edu).
[8]Authors contributed equally to this work

Author Contributions
A.L.B. designed and performed RNAi screen and all validation experiments qRT-PCR, generation of stable cell lines and studies on cyclosporin, cholesterol and trichostatin. A.R. designed and performed metabolite experiments and histone acetylation study. S.L.S. participated in the design of the overall study and S.H., D.E.I. and S.L.S. contributed to the preparation of the manuscript. D.E.I. and A.L.B. conceived of the idea for this study. All authors interpreted data, commented on results, and participated in writing the manuscript.

Competing Financial Interests
The authors declare no competing financial interests.

Numerous studies have pointed to the central role of transcription factors in cell differentiation (1). We sought to determine if carbon metabolism is connected to the cellular differentiation network (2) and, if so, whether it could provide a novel method for controlling myogenic differentiation. Here, we provide evidence that perturbations at specific points in the metabolic network can induce muscle myoblasts to differentiate into myosin heavy chain-expressing myotubes and we elucidate the associated metabolic pathways. We show that this finding can be applied to small molecule-based differentiation of human rhabdomyo-sarcoma cells.

We developed a method for RNAi-based screening using mouse C2C12 myoblasts. These cells are proliferative in the presence of serum (10% fetal bovine serum (FBS)) and can be induced to differentiate into multi-nucleated myotubes by serum withdrawal within 5 days (3). To determine whether metabolic enzymes play a role in inducing muscle differentiation, we performed a phenotypic, high-content screen by knocking down 50 enzymes of carbon catabolism using short hairpin RNAs (Supplementary Table 1) in the presence of 10% FBS (Supplementary Methods). Differentiation induced by the hairpins was quantitated by image analysis of myosin heavy chain expression using immunofluorescence. Integrated myosin heavy chain intensity per well was calculated relative to that in control wells. Negative controls included cells infected with non-targeting hairpins (e.g. shLacz, shRFP and shGFP), and positive control cells were treated with 2% horse serum (HS), which induces differentiation (3). Three enzymes were identified that induced the differentiation of C2C12 myoblasts following knockdown: phosphoglycerate kinase (Pgk1), hexose-6-phosphate dehydrogenase (H6pd) and ATP citrate lyase (Acl) (Figure 1a–b). Successful knockdown by at least two distinct shRNAs targeting each of these metabolic genes and expression of various differentiation markers (myogenin and myosin heavy chain) were confirmed by Western blot analysis and quantitative RT-PCR, respectively (Supplementary Figure 1a–g). We further confirmed the on-target effects of Pgk1 and H6pd knockdown by establishing cell lines stably expressing the human orthologs of Pgk1 and H6pd. Knockdown of the endogenous mouse genes in these cell lines failed to induce differentiation (Supplementary Figure 1h).

Because some metabolic enzymes have been shown to possess metabolism-independent regulatory functions (4) we next determined whether myogenic differentiation was accompanied by changes in levels of the metabolites regulated by, Pgk1, H6pd and Acl. We analyzed global changes in levels of intracellular metabolites that accompany myogenic differentiation using LC-MS/MS-based metabolic profiling (Supplementary Methods). Myogenic differentiation was induced by culturing C2C12 cells in reduced serum, and relative levels of intracellular metabolites were measured on days 0, 3 and 6 after initiating differentiation (complete list of measurements is provided in Supplementary Table 2). Upon differentiation, two salient changes were observed: 1) a decrease in glycolytic intermediates 3-phosphoglycerate and phosphoenol pyruvate and 2) a decrease in the bile acids taurodeoxycholic acid (TUDCA) and glycochenodeoxycholic acid (Supplementary Figure 1i). Pgk1 catalyzes the formation of 3-phosphoglycerate, which is then metabolized to phosphoenol pyruvate during glycolysis. Both of these metabolites were found to decrease significantly during myogenic differentiation. Bile acids including TUDCA are endogenous

inhibitors of endoplasmic reticulum (ER)-based stress (5). H6pd is an ER-localized isoform of glucose 6-phosphate dehydrogenase, and inhibition of H6pd causes ER stress *in vivo* (6).

Previous studies suggest that ER signaling can activate the calcium/calcineurin/NFAT pathway; both ER stress and NFAT signaling via the phosphatase calcineurin are known mediators of skeletal muscle differentiation and function (7–9). We found that H6pd induces differentiation of C2C12 cells in a calcineurin-dependent fashion (Figure 1c) as judged by the inhibition of differentiation upon treatment with cyclosporin A (CsA). This effect was specific for shH6pd and not seen with shPgk1 or shAcl (Figure 1c). Thus, we infer that H6pd knockdown promotes myogenic differentiation through an ER-signaling mechanism that is dependent on calcineurin.

We were unable to identify metabolites from the metabolic profile that reveal a direct role for Acl, the third enzyme identified in the RNAi screen. Therefore, we separately examined whether Acl impacts differentiation via its downstream effects on metabolism. Acl is a primary source of nuclear acetyl coA for histone acetylation (10) and cytoplasmic acetyl CoA for cholesterol and fatty acid synthesis (11). We explored the effect of Acl knockdown in C2C12 cells on both of these pathways.

We determined that C2C12 differentiation by Acl knockdown is dependent on histone deacetylases (HDACs), as judged by the inhibition of shAcl-mediated differentiation by the HDAC inhibitor trichostatin A (TSA) (Figure 1d). We hypothesized that depletion of Acl would reduce nuclear acetyl coA, which is a necessary cofactor for histone acetyl transferases. We therefore measured levels of histone acetylation in shAcl-treated cells (10) and found that knockdown of Acl reduces levels of acetylated histones (Figure 1e). This suggests a mechanistic connection between acetyl CoA metabolism, chromatin and myogenic differentiation.

Our primary screen indicated that lipid metabolism per se was not an effector of differentiation since knockdown of enzymes in fatty acid s-oxidation did not cause myoblast differentiation. We therefore examined the role of cholesterol metabolism by treating cells with statins, small-molecule inhibitors of cholesterol biosynthesis, and found that they stimulate differentiation. C2C12 myoblasts were treated with three different statins: pravastatin, atorvastatin and fluvastatin. Fluvastatin and atorvastatin are potent inducers of C2C12 differentiation (at 1 μM), while pravastatin is less effective but also capable of inducing myogenic differentiation (Supplementary Figure 2a, b). Furthermore, cholesterol abrogates the differentiation-promoting effect of statins, suggesting that cholesterol mediates C2C12 differentiation (Supplementary Figure 2c). We have observed that both cholesterol and TSA inhibit differentiation induced by serum withdrawal (Supplementary Figure 2d), implicating both the nuclear and cytoplasmic acetyl coA in myoblast differentiation.

Treatment of the human RD embryonal rhabdomyosarcoma cell line with fluvastatin induced rhabdomyosarcoma cell differentiation, reduced cancer cell proliferation and inhibited anchorage-independent growth (Figure 2a–c, Supplementary Figure 2e, Supplementary Methods). Rhabdomyosarcoma is the most common pediatric soft-tissue sarcoma and is presumed to derive from cells of the skeletal muscle lineage (12).

Interference with any of three key nodes of the metabolic network described herein may offer new approaches to cancer differentiation therapy for rhabdomyosarcoma.

In this study, we identify three novel metabolic enzymes whose knockdown with RNAi causes myoblast differentiation: Pgk1, H6pd and Acl. During myogenic differentiation, Pgk1 mRNA levels decrease by about 50% within 4 days after proliferating cells are induced to differentiate (13). We provide evidence that metabolic intermediates regulated by Pgk1, 3-phosphoglycerate and phosphoenol pyruvate decrease during myogenic differentiation.

Unlike its cytosolic isoform glucose-6-phosphate dehydrogenase, H6pd localizes to the ER and is used to regenerate reduced nicotinamide adenine dinucleotide phosphate (NADPH) within the ER when glucose-6-phosphate and NADP are available (14, 15). H6pd-null mice develop skeletal myopathy characterized by switching of type-II fibers to type-I (slow) fibers. The absence of H6pd impairs protein folding and activates the unfolded protein response pathway (6). Here we show that H6pd knockdown induces myoblast differentiation, and that myogenic differentiation is accompanied by a decrease in endogenous inhibitors of ER stress: the bile acids, TUDCA and glycochenodeoxy-cholic acid. Further, we provide a mechanistic connection between H6pd, ER stress and calcium/calcineurin signaling by showing that CsA overcomes shH6pd-mediated differentiation.

Acl catalyzes the synthesis of acetyl-CoA, which is used in nuclear histone acetylation and cytoplasmic cholesterol biosynthesis. We provide evidence that both pathways are relevant to shAcl-mediated differentiation. Inhibition of Acl reduces global chromatin acetylation (10). Similarly, we found a decrease in chromatin acetylation following Acl knockdown. However, the differentiation response elicited by shAcl appears to be cell-context specific. In pre-adipocytes, shAcl blocks differentiation (10) whereas and in myoblasts, it induces differentiation (as shown in this report). In cancer models, inhibition of Acl by either RNAi or the small molecule SB-204990 limits proliferation and survival of tumor cells displaying aerobic glycolysis *in vitro* (16), and induces tumor differentiation and reduction in tumor growth *in vivo* (16). We show here that inhibition of cholesterol metabolism through treatment with fluvastatin induces rhabdomyosarcoma cell differentiation, blocks proliferation and prevents anchorage-independent growth.

Thus, we discovered that myogenic differentiation and cellular metabolism are coordinated via at least three cellular pathways: calcium/calcineurin signaling, chromatin acetylation and the cholesterol biosynthetic pathway. These data suggest that metabolic enzymes may be important for the control of cancer cell growth and differentiation, and that metabolic perturbations may result in important changes in cell states. Alterations in the metabolic network identified herein may serve as novel therapeutic approaches to muscle sarcoma differentiation therapy in the future.

Supplementary Material

Refer to Web version on PubMed Central for supplementary material.

Acknowledgments

References

1. Loh YH, Ng JH, Ng HH. Cell Cycle. 2008; 7:885–91. [PubMed: 18414030]

2. Bolouri H, Davidson EH. Dev Biol. 2002; 246:2–13. [PubMed: 12027430]

3. Yaffe D, Saxel O. Differentiation. 1977; 7:159–66. [PubMed: 558123]

4. Popanda O, Fox G, Thielmann HW. Biochim Biophys Acta. 1998; 1397:102–17. [PubMed: 9545551]

5. Ozcan U, et al. Science. 2006; 313:1137–40. [PubMed: 16931765]

6. Lavery GG, et al. J Biol Chem. 2008; 283:8453–61. [PubMed: 18222920]

7. Nakanishi K, Dohmae N, Morishima N. FASEB J. 2007; 21:2994–3003. [PubMed: 17435177]

8. Tomida T, et al. EMBO J. 2003; 22:3825–3832. [PubMed: 12881417]

9. Schulz RA, Yutzey KE. Dev Biol. 2004; 266:1–16. [PubMed: 14729474]

10. Wellen KE, et al. Science. 2009; 324:1021–2. [PubMed: 19460991]

11. Beigneux AP, et al. J Biol Chem. 2004; 10:9557–64. [PubMed: 14662765]

12. Dagher R, Helman L. Oncologist. 1999; 4:34–44. [PubMed: 10337369]

13. Tomczak KK, et al. FASEB J. 2004; 18:403–5. [PubMed: 14688207]

14. Barash V, Erlich T, Bashan N. Biochem Int. 1990; 20:267–74. [PubMed: 2156506]

15. Hewitt KN, Walker EA, Stewart PM. Endocrinology. 2005; 146:2539–43. [PubMed: 15774558]

16. Hatzivassiliou G, et al. Cancer Cell. 2005; 8:311–21. [PubMed: 16226706]
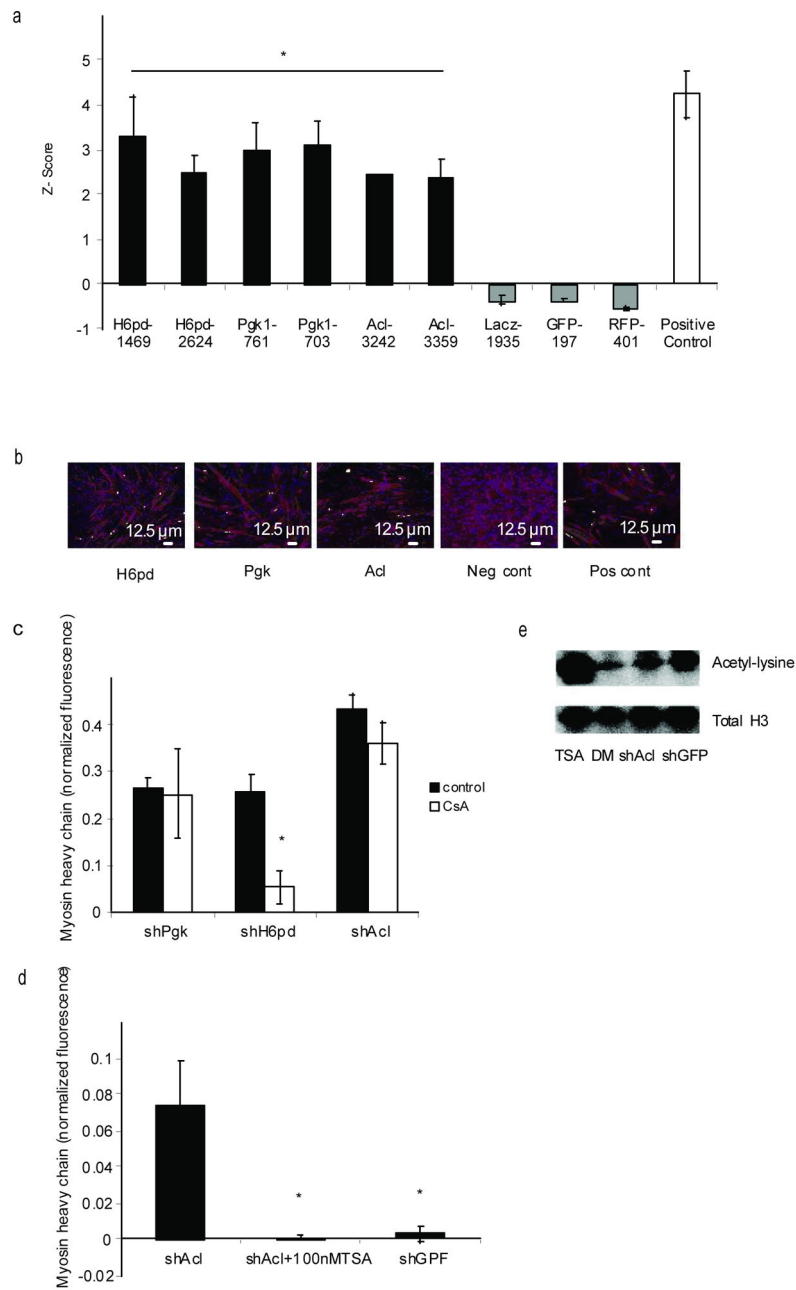
Figure 1.
Figure 1a–e. RNAi screen and effects of cyclosporin (CsA) and trichostatin (TSA) on
C2C12 differentiation. Knockdown of Pgk1, Acl and H6pd causes myoblast differentiation
(a) Immunofluorescence of myosin heavy chain expression. The myosin heavy chain
fluorescence intensity was normalized to the integrated fluorescence intensity of Hoechst
nuclear stain. Significant changes in levels of myosin heavy chain expression relative to
control hairpins were calculated as Z scores (* Z score > 2.6). The entire screen was
performed three independent times. Error bars represent standard error of the mean. (b)
Images show formation of multi-nucleated myotubes and increased myosin heavy chain
intensity upon shRNA knockdown. Cells cultured in 2% horse serum served as positive

controls for differentiation. (c) CsA treatment inhibits C2C12 differentiation induced by shH6pd. Cells were infected with shAcl, shH6pd or shPgk1. Following gene knockdown, cells were cultured for three days in 0.1 ug/ml cyclosporin (CsA). Data represent three independent experiments performed in triplicate. Error bars represent standard error of the mean, P-value < 0.05. (d) TSA treatment inhibits C2C12 differentiation. 100nM TSA is sufficient to block differentiation initiated by shAcl. (e) Western blot analysis depicts changes in histone acetylation upon overnight treatment with TSA (500 nM), positive control, DM cells were cultured for three days in differentiation medium, and hairpin-infected cells were harvested 48 hours post-infection, shAcl and shGFP.
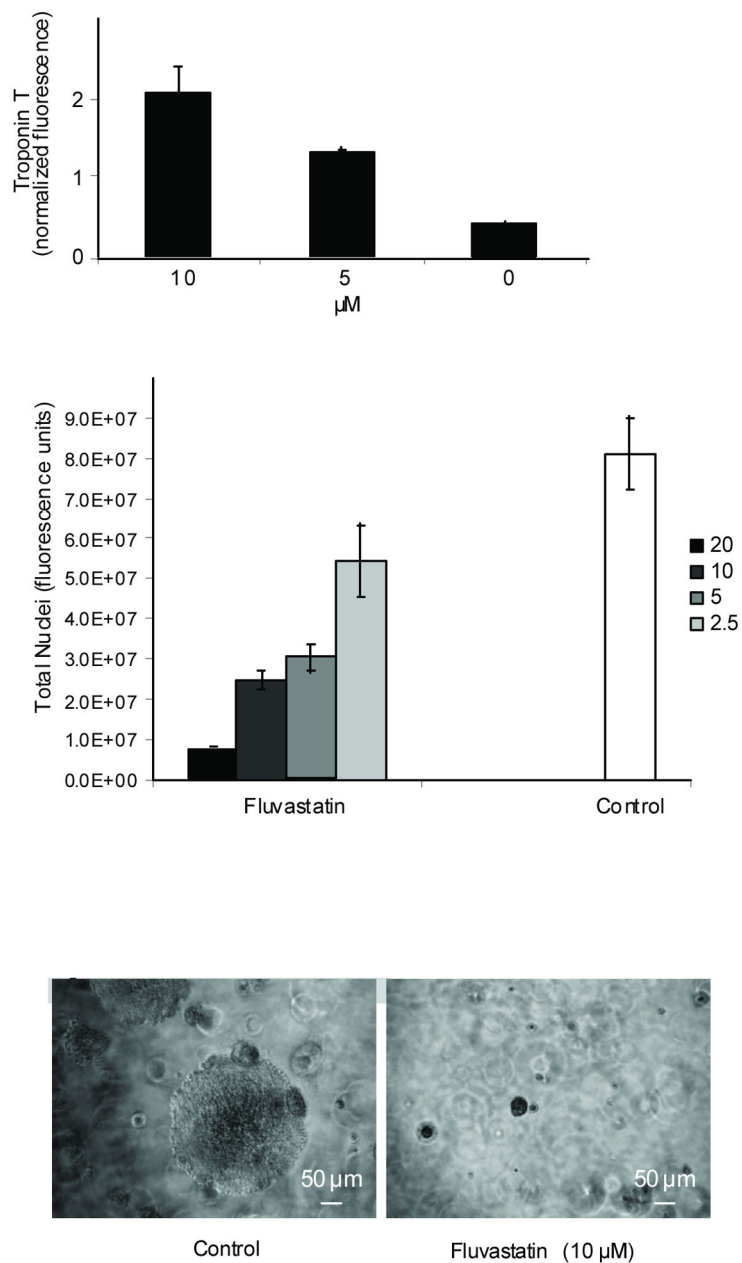
Figure 2.
Figure 2a–c. Fluvastatin treatment causes differentiation of human rhabdomyo-sarcoma cells and inhibits their proliferation and growth on soft agar. (a) RD human rhabdomyosarcoma cells were treated with fluvastatin in normal growth media for four days. Cells were fixed and stained for troponin T expression. Immunofluorescence was normalized to Hoechst nuclear stain. (*P-value < 0.05 t-test) (b) Fluvastatin inhibits human rhabdomyosarcoma cell proliferation. RD rhabdomyosarcoma cells were plated in triplicate. Cells were treated with increasing doses of fluvastatin 2.5–20 μM for four days. Cells were fixed and nuclei were stained with Hoechst dye. Total nuclear fluorescence intensity was quantitated as a measure of cell proliferation. (c) Fluvastatin prevents rhabdomyosarcoma growth on soft agar. Cells

were grown in triplicate on soft agar and treated with 10 μM fluvastatin. Images were captured 14 days post-seeding.

Figure 3.